JOURNAL OF VIROLOGY, May 2011, p. 4720–4729 Vol. 85, No. 10
0022-538X/11/$12.00 doi:10.1128/JVI.02032-10

Human Adenovirus Type 5 Induces Cell Lysis through Autophagy and Autophagy-Triggered Caspase Activity▽

Hong Jiang,[1]* Erin J. White,[1] Christian I. Ríos-Vicil,[2] Jing Xu,[1] Candelaria Gomez-Manzano,[1] and Juan Fueyo[1]

Brain Tumor Center, The University of Texas M. D. Anderson Cancer Center, Houston, Texas 77030,[1] and University of Puerto Rico, Medical Sciences Campus, School of Medicine, San Juan, Puerto Rico 00936[2]

Received 24 September 2010/Accepted 23 February 2011

Oncolytic adenoviruses, such as Delta-24-RGD, are promising therapies for patients with brain tumor. Clinical trials have shown that the potency of these cancer-selective adenoviruses should be increased to optimize therapeutic efficacy. One potential strategy is to increase the efficiency of adenovirus-induced cell lysis, a mechanism that has not been clearly described. In this study, for the first time, we report that autophagy plays a role in adenovirus-induced cell lysis. At the late stage after adenovirus infection, numerous autophagic vacuoles accompany the disruption of cellular structure, leading to cell lysis. The virus induces a complete autophagic process from autophagosome initiation to its turnover through fusion with the lysosome although the formation of the autophagosome is sufficient for virally induced cell lysis. Importantly, down-modulation of autophagy genes (*ATG5* or *ATG10*) rescues the infected cells from being lysed by the virus. Moreover, autophagy triggers caspase activity via the extrinsic FADD/caspase 8 pathway, which also contributes to adenovirus-mediated cell lysis. Therefore, our study implicates autophagy and caspase activation as part of the mechanism for cell lysis induced by adenovirus and suggests that manipulation of the process is a potential strategy to optimize clinical efficacy of oncolytic adenoviruses.

We reported previously the antiglioma effect of the E1A mutant oncolytic adenovirus Delta-24, which is targeted to the aberrant Rb/E2F1 pathway in cancer cells (10). In subsequent reports, we described how Delta-24-RGD, a version of Delta-24 whose infectivity in cancer cells is enhanced through insertion of an RGD-4C motif in the HI loop of the adenoviral fiber protein (37), showed oncolytic potency in intracranial models of human glioma xenografts derived from both malignant glioma cell lines (9) and brain tumor stem cells (15). On the basis of these preliminary data and toxicity studies performed under the guidance of the National Cancer Institute, we have translated Delta-24-RGD to the clinical setting, and it is currently being tested for toxicity in patients with recurrent malignant glioma at The University of Texas M. D. Anderson Cancer Center. Although we anticipate that the studies will show negligible toxicity, we expect that further improvements in the oncolytic potency of Delta-24-RGD will be necessary to induce optimal therapeutic effect. One of the potential avenues to increasing adenovirus potency that remains understudied is the mechanism by which adenoviruses induce cell lysis. In this regard, we along with other groups have shown that adenovirus infection results in macroautophagy (here referred to as autophagy) (12, 15, 41). Although it has been suggested that this cellular process might be linked to adenovirus-induced cell lysis (17), the underlying mechanism is still largely unknown.

Autophagy is a dynamic cellular process that degrades damaged or obsolete organelles and proteins (34, 43). The process uses specialized cytosolic vesicles to engulf cytoplasmic components and ultimately fuse with the lysosome to digest the macromolecules for recycling (43). In addition to its role in cellular homeostasis, autophagy acts as a cellular response to stresses such as starvation or pathogen infection (13, 22). Although autophagy in most scenarios is believed to promote cell survival, accumulating evidence indicates that, under certain pathological situations, autophagy can also trigger and mediate type II programmed cell death (3). The transition of autophagy to autophagic cell death involves recruitment of Fas-associated death domain protein (FADD) to the autophagic membrane structure and activation of caspase 8 (33).

When cells are attacked by pathogens, the invading microbes can be rapidly sequestered into autophagosomes and thus degraded in the cell through autophagy (29). However, some RNA viruses may subvert the defensive function of autophagy and use the autophagic double-membrane vesicles as a scaffold for the replication complex (14, 42). Viruses may also use autophagy-related vacuoles as a means for the new progeny to exit the infected cell (14). For instance, poliovirus may be engulfed by autophagosomes and released from cells after fusion of lysosomes with the plasma membrane (14). Adenoviruses, at the end of the infectious cycle, induce lysis of the host cell to release viral progeny (4). So far, this process of cell death has not been clearly documented. Abou El Hassan et al. reported in 2004 that adenoviruses induce cell death via a basic apoptotic machinery-independent mechanism that resembles necrosis-like programmed cell death (1). More recently, this type of cell death was further suggested to be autophagic cell death (12, 15). Therefore, we speculate that adenoviruses may induce autophagy to activate host cell lysis process and thus

* Corresponding author. Mailing address: Department of Neuro-Oncology, Unit 1002, The University of Texas M. D. Anderson Cancer Center, 1515 Holcombe Blvd., Houston, TX 77030. Phone: (713) 834-6203. Fax: (713) 834-6230. E-mail: hjiang@mdanderson.org.

▽ Published ahead of print on 2 March 2011.

facilitate viral progeny release at the end of the infectious cycle.

In this report, we describe our studies of various cells infected with Delta-24-RGD and wild-type human adenovirus serum type 5 (Ad5) and present evidence that the viruses induce complete autophagy flux accompanying the lysis of the host cell. Further, we demonstrate that autophagy plays a role in the cytolysis process and triggers caspase activity through the FADD/caspase 8 pathway, which collaborates with the autophagy process to lyse the host cell.

MATERIALS AND METHODS

Cell lines and culture conditions. Human glioblastoma-astrocytoma U-87 MG and U-251 MG cells and human lung fibroblast MRC-5 cells (American Type Culture Collection, Manassas, VA) were cultured in Dulbecco's modified Eagle's medium-nutrient mixture F12 (DMEM/F12) supplemented with 10% fetal bovine serum (FBS; HyClone Laboratories, Inc., Logan, UT), 100 μg/ml penicillin, and 100 μg/ml streptomycin (Invitrogen, Carlsbad, CA). Human leukemia cell lines A3, I2.1, and I9.2 (American Type Culture Collection) were grown in RPMI 1640 medium supplemented with 10% FBS and antibiotics. Wild-type (wt) and *ATG5* knockout (*ATG5*$^{-/-}$) mouse embryo fibroblasts (MEFs; generous gifts from N. Mizushima, Tokyo Medical and Dental University, Tokyo, Japan) (21) were maintained in DMEM supplemented with 5% FBS and antibiotics. The cells were kept at 37°C in a humidified atmosphere containing 5% CO_2.

Reagents and antibodies. Acridine orange, bafilomycin A1 (BA1), rapamycin (Rapa), and 3-methyladenine (3-MA) were obtained from Sigma-Aldrich (St. Louis, MO). Antibodies used in the studies were as follows: goat polyclonal anti-actin (I-19), rabbit polyclonal anti-E1A, and mouse monoclonal anti-p62 (SQSTM1/sequestosome 1) from Santa Cruz Biotechnology (Santa Cruz, CA); rabbit polyclonal anti-LC3B (where LC3B is an isoform of the autophagy marker protein light chain 3), anti-PARP1 [where PARP1 is poly-(ADP-ribose) polymerase 1], and mouse monoclonal anti-caspase 8 from Cell Signaling Technology (Danvers, MA); mouse monoclonal anti-α-tubulin (B-5-1-2) from Sigma-Aldrich; rabbit polyclonal anti-Atg5 from Cosmo Bio Co., Ltd. (Tokyo, Japan); and mouse monoclonal anti-Atg10 from MBL International Corp. (Woburn, MA).

Adenovirus. The adenoviruses used in the studies were human serum type 5 (Ad5), including the replication-deficient adenoviral vector AdCMV (where CMV is cytomegalovirus), an adenoviral vector expressing green fluorescent protein (GFP) with RGD-modified fiber (AdGFP-RGD) (25), wild-type Ad5 (Adwt) (18), and replication-competent adenovirus Delta-24-RGD (9, 36) (prepared by the Keck Institutional Vector Core Facility at M. D. Anderson Cancer Center). Delta-24-RGD encompasses an 8-amino-acid deletion in the CR-2 region of E1A protein and an insertion of an RGD-4C motif in the HI loop of the fiber protein (9, 36). The viruses were amplified in 293 (AdCMV and AdGFP-RGD) or A549 (Adwt and Delta-24-RGD) cells, purified by three successive bandings on cesium, and stored at −80°C. The viral titer was assayed with a Adeno-X-Rapid Titer Kit (Clontech, Mountain View, CA) and determined as PFU/ml. The virus particle/PFU ratios were less than 50.

Subcellular localization of EGFP-mCherry-LC3 fusion protein. U-87 MG cells were transfected with an enhanced GFP (EGFP)-mCherry-LC3 fusion protein-expressing plasmid (a kind gift from T. Johansen, University of Tromso, Norway) (31) by FuGENE 6 (Roche Molecular Biochemicals, Indianapolis, IN). Images of live cells were taken and processed on a Zeiss Axiovert Zoom fluorescence microscope (Carl Zeiss, Inc., Thornwood, NY) equipped with an AxioCam MRM camera and a 40× (1.3 numerical aperture) oil EC Plan-Neofluar objective, using Immersol (refractive index, 1.518) at room temperature. Acquisition software was AxioVision, release 4.7.1 (Carl Zeiss, Inc.). Image processing (i.e., proportional adjustments) was done by Photoshop (Adobe, San Jose, CA).

EM. Cell samples were fixed with a solution containing 3% glutaraldehyde plus 2% paraformaldehyde in 0.1 M cacodylate buffer (pH 7.3) for 1 h. After fixation, the samples were washed and treated with 0.1% Millipore-filtered cacodylate-buffered tannic acid, postfixed for 1 h with 1% buffered osmium tetroxide, and then stained with 1% Millipore-filtered uranyl acetate (all from Sigma-Aldrich). The samples were dehydrated in increasing concentrations of ethanol, infiltrated, and then embedded in Spurr's low-viscosity medium. They were then polymerized in an oven for 2 days at 70°C. Ultrathin sections were cut in a Leica Ultracut microtome (Leica, Deerfield, IL), stained with uranyl acetate and lead citrate in a Leica electron microscopy (EM) stainer, and examined using a JEM-1010 transmission electron microscope (JEOL USA, Inc., Peabody, MA) at an accelerating voltage of 80 kV. Digital images were obtained using an imaging system from Advanced Microscopy Techniques (Danvers, MA).

Quantification of acidic vesicular organelles with acridine orange staining. Acridine orange staining of the cells was conducted as described previously (15). Briefly, 1.0 μg/ml acridine orange was added to the cell culture, and the cells were incubated for 15 min. Stained cells were then analyzed by flow cytometry using a FACScan cytometer and CellQuest software (both from Becton Dickinson, San Jose, CA). Red (FL3-H channel) fluorescence emissions from 10^4 cells were analyzed.

Quantification of cell lysis. Cells were stained with 8 μM ethidium homodimer 1 (Molecular Probes, Inc., Eugene, OR) in phosphate-buffered saline (PBS) solution for 15 min at room temperature. Stained cells were then analyzed by flow cytometry using a FACScan cytometer and CellQuest software (Becton Dickinson). Red (FL2-H channel) fluorescence emissions from 10^4 cells were analyzed. Unless specifically indicated, cell lysis was assayed with this method throughout the work.

Lysed cells were also accessed by trypan blue exclusion. Briefly, cells were suspended in PBS and mixed with an equal volume of 0.4% trypan blue (Invitrogen) for 3 min. The unstained (viable) and stained (lysed) cells were counted with a hemacytometer within 3 to 5 min.

Immunoblotting. The cells were collected and resuspended in PBS plus protease inhibitor cocktail (Sigma-Aldrich) and then subjected to lysis by the addition of an equal volume of 2× sodium dodecyl sulfate loading buffer. Afterward, the lysates were heated at 95°C for 10 min. Equal amounts of proteins from the lysates were separated by sodium dodecyl sulfate-polyacrylamide gel electrophoresis, transferred to a nitrocellulose membrane, and probed with antibodies. Finally, the protein bands were visualized using an ECL Western blot detection system (Amersham Pharmacia Biotech, Piscataway, NJ).

RNA interference. To knock down *ATG5* and *ATG10*, we purchased small hairpin RNA (shRNA)-expressing plasmids from Origene (Rockville, MD). We transferred the plasmids into the cells with FuGENE 6. The cells were screened, and stable cell clones were maintained in culture medium plus 0.5 μg/ml puromycin.

Virus replication assay. Cells were seeded at a density of 5×10^4 cells/well in 12-well plates and infected with Delta-24-RGD at 10 PFU/cell. Forty-eight hours after infection, the titers of the infectious viral progeny were determined using an Adeno-X-Rapid Titer Kit (Clontech) according to the manufacturer's instructions. Final viral titers were determined as PFU/ml.

Isolation of mitochondria. Mitochondria were isolated from cells (2×10^7 cells) with a Mitochondria Isolation Kit for culture cells (Thermo Scientific, Rockford, IL) according to the instructions from the manufacturer.

Statistical analyses. A two-tailed Student's *t* test was used to determine the statistical significance of the results of our experiments. *P* values of <0.05 were considered statistically significant. For these studies, data are given as means ± standard deviations (SD).

RESULTS

Development of autophagy accompanies destruction of cellular structures and release of adenoviral progenies. To examine the correlation of autophagy and cell lysis induced by adenoviruses, we infected human malignant glioma U-251 MG cells with Delta-24-RGD virus and human lung fibroblast MRC-5 cells with wild-type Ad5 and monitored the infection cycle. During a 5-day infection period, the cell population demonstrated a progressive accumulation of autophagic vacuoles in the cytoplasm and destruction of cellular structures (Fig. 1A and B). At 72 h after viral infection, we observed numerous autophagic vacuoles in the cytoplasm of infected cells but not uninfected cells (Fig. 1, frames a and b). Some of the vacuoles encompassed cytoplasmic content (Fig. 1, frames c), such as membrane structures from cellular organelles, but the nuclei were still intact (Fig. 1, frames b). The autophagic features were coincident with the presence of viral protein crystal (inclusion body) and assembled virions (Fig. 1, frames c).

With progression of the infection (96 h after viral infection), autophagic vacuoles were more numerous and covered a greater part of the cytoplasm (Fig. 1, frames d). The impressive

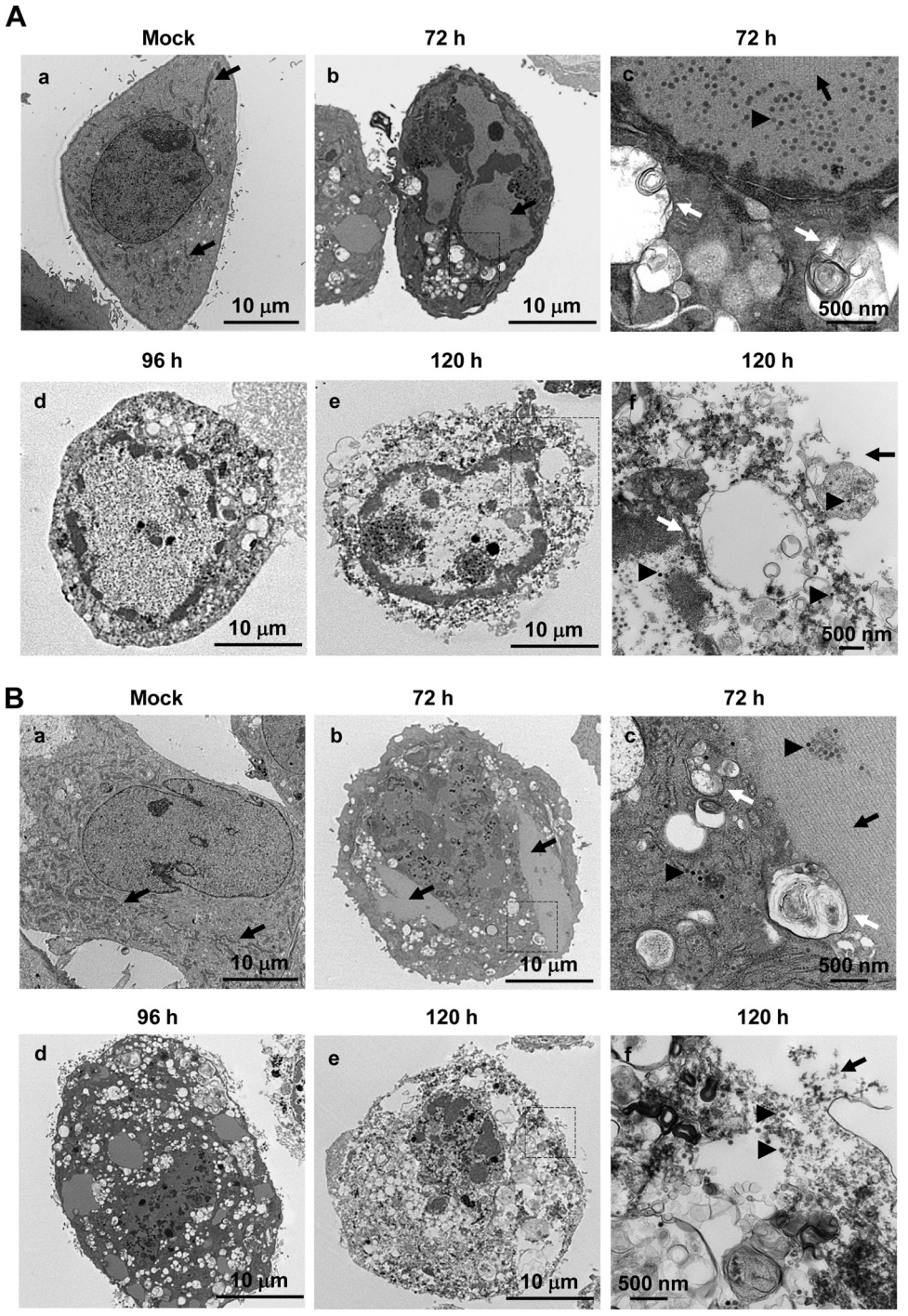

FIG. 1. Representative electron micrographs show progressive development of autophagy and cell lysis in Delta-24-RGD-infected U-251 MG cells (A) and wild-type adenovirus 5 (Adwt)-infected MRC-5 cells (B). Cells were mock infected or infected with Delta-24-RGD or Adwt at a dose of 10 PFU/cell and examined at 72, 96, and 120 hours after infection, as indicated on the figure. Note that numerous mitochondria appear in mock-infected cells (arrows) but are barely seen in the cells after 96 h postinfection. Frame c in each panel is a close-up of a part of the cell in frame b showing vesicles in the cytoplasm (white arrows) and virions (arrowhead) clustered along or within an inclusion body (black arrow). Frame f in each panel is a close-up of a part of the cell in frame e revealing numerous vacuoles together with a discontinuous nuclear membrane (white arrow in panel A, frame f) and cellular membrane (black arrows) through which viral progeny (arrowheads) burst out of the disrupted cytoplasm.

vacuolization of the cytoplasm was accompanied by a decrease in the number of organelles, with very few visible mitochondria. Despite the fragile aspect of the cytoplasm, the nuclear membrane seemed to be intact. The cell membrane was also preserved, and cell morphology was maintained. At a later time point (120 h after viral infection), tremendous disruption of the cellular membrane accompanied a heavily vacuolated cytoplasm and destruction of structures in the cell (Fig. 1,

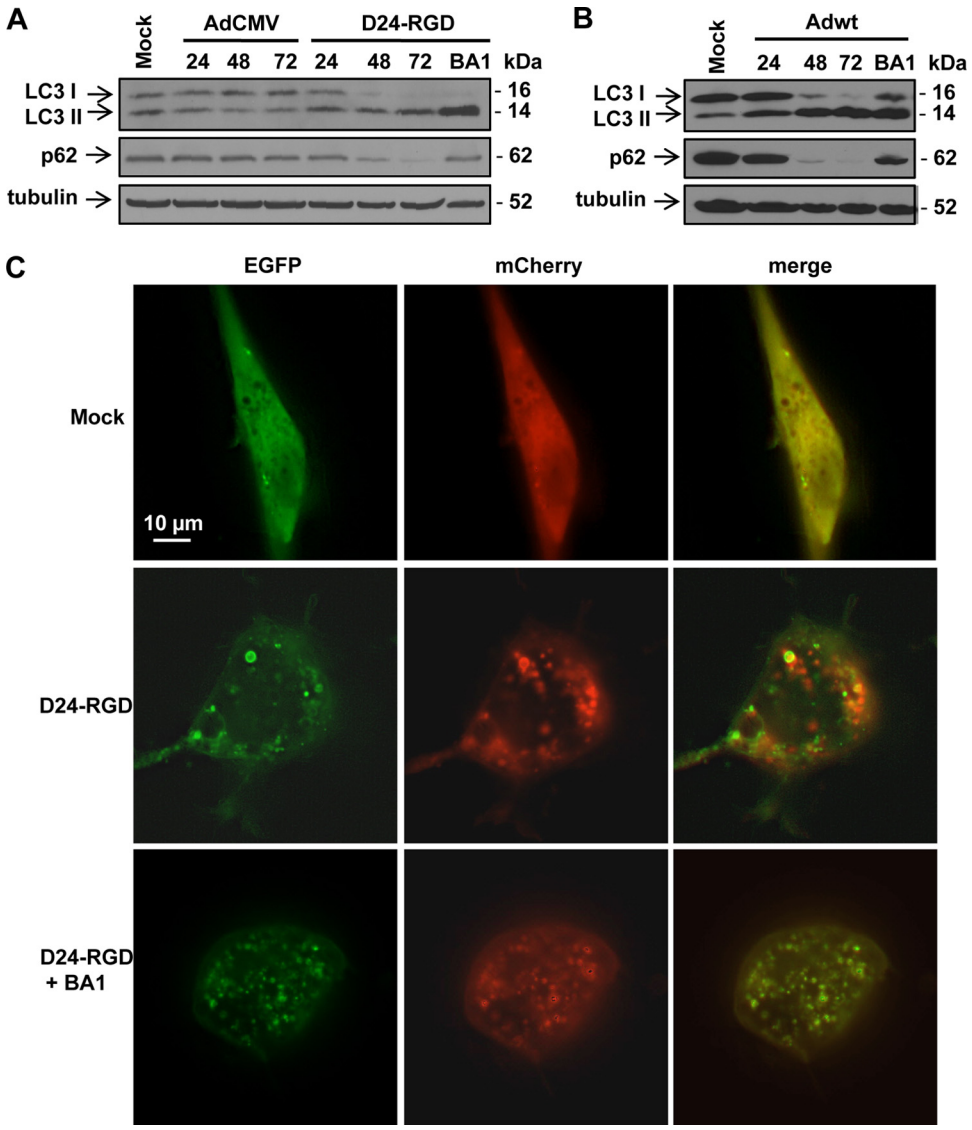

FIG. 2. Adenovirus induces a complete autophagic flux. (A) U-87 MG cells were infected with replication-deficient adenoviral vector AdCMV (10 PFU/cell) and Delta-24-RGD (D24-RGD; 10 PFU/cell). (B) U-251 MG cells were infected with Adwt (10 PFU/cell). Cells were collected at 24, 48, and 72 h after infection. Bafilomycin A1 (BA1; 10 nM) was added to the cells 24 h after viral infection, and cells were collected 48 h later. Cell lysates were subjected to immunoblot analysis. Tubulin expression was used as a loading control. (C) Representative images of mCherry-EGFP-LC3 fluorescence in the U-87-MG cells. Cells were first transfected with plasmid expressing mCherry-EGFP-LC3. Twenty-four hours later, cells were infected with Delta-24-RGD at 50 PFU/cell in the absence or presence of 10 nM bafilomycin A1. After 48 h, live cells were observed under fluorescence microscopy.

frames e and f). The continuity of the nuclear membrane was finally broken (Fig.1 Af), allowing the virions to escape from the nucleus into the destroyed cytoplasm and release of virus progenies from the cells (Fig. 1, frames f). Taken together, the timeline of these events suggests that progression of autophagy in the cytoplasm occurs during the adenoviral infection cycle and coexists with assembly of viral particles. These data also provide a rationale for speculation that autophagy plays a role in degeneration of the cytoplasm, leading to cell lysis and subsequent release of new viral progenies.

Adenovirus induces complete autophagic flux. The autophagy process features a flux from initiation of the autophagosome to its maturation through fusion with the lysosome to form the autolysosome, resulting in its final turnover (20). Because accumulation of autophagosomes in the cytoplasm is due to either an increased rate of autophagosome initiation or a decreased rate of autophagosome turnover, we next examined the autophagy flux induced by Delta-24-RGD and wild-type Ad5. First, we performed a time course study during viral infection in human glioma U-87 MG cells and U-251 MG cells. From 48 to 72 h after viral infection, conversion of LC3-I to LC3-II was upregulated (Fig. 2A and B), indicating activation of the autophagy cascade and formation of autophagosomes. Meanwhile, levels of p62, a long-lived protein that is degraded through autophagy (27), decreased dramatically, suggesting that autophagosomes were able to fuse with lysosomes (mat-

uration to form autolysosomes) to degrade the cargo proteins. When this fusion process was inhibited by bafilomycin A1, an inhibitor of vacuolar ATPase (8), however, both LC3-II and p62, which can be degraded by hydrolases from lysosomes, accumulated in the cells.

Next, we took advantage of a double-tagged EGFP-mCherry-LC3 construct (31), which is detected as yellow fluorescence (green merged with red) in nonacidic structures (autophagosomes and amphisomes) and as red only in autolysosomes because of quenching of the EGFP in these acidic structures. Thus, the color of the fluorescence indicates the stage of the autophagy process. By expressing EGFP-mCherry-LC3 in the Delta-24-RGD-infected cells, we were able to visualize LC3 both in acidic vesicles displaying red fluorescence and in neutral structures displaying yellow fluorescence (Fig. 2C), suggesting that the virus induced both the initiation and maturation of autophagosomes but did not stop the process at the autophagosome stage. When bafilomycin A1 was added as a technical control to adenovirus-infected cells, all the vacuoles were yellow (Fig. 2C). These data clearly indicate that adenovirus induces a complete autophagy process, from initiation of the autophagosome to fusion with the lysosome, which results in its turnover.

Autophagosome formation is sufficient for host cell lysis by Delta-24-RGD. Next, we asked how autophagy flux is involved in the process of cell lysis induced by Delta-24-RGD. For this study, we used two autophagy inhibitors that target different stages of the autophagy flux. 3-Methyladenine (3-MA) inhibits phosphoinositide 3-kinase (PI3K) class III that positively regulates autophagic sequestration at autophagy initiation (24, 32). Bafilomycin A1 inhibits the fusion of the autophagosome and lysosome (8). Addition of 3-MA to adenovirus-infected cells substantially inhibited autophagy in the cells, as indicated by decreases in the percentages of cells with acidic vesicle organelles (AVOs), a cellular marker of autophagy (30), from 19.5% ± 0.5% to 7.8% ± 1.0% (Fig. 3A). This treatment partially rescued the cells from adenovirus-mediated cell lysis, as indicated by staining of DNA in cells with broken membranes by the DNA fluorescence dye ethidium homodimer 1 (reduction in lysis from 27.4% ± 1.4% to 19.7% ± 0.3%) (Fig. 3B), which was consistent with the cell lysis assayed by trypan blue exclusion (Fig. 3C). However, although bafilomycin A1 blocked all the AVO formation in the cells (Fig. 3D), it could not rescue the cells from being lysed by Delta-24-RGD (Fig. 3E). In contrast, rapamycin, a classical autophagy inducer (34), enhanced the AVOs (from 32.9% ± 2.1% to 47.8% ± 3.0%) (Fig. 3F) and the cell lysis (from 33.0% ± 0.9% to 41.4% ± 1.2%) (Fig. 3G) induced by Delta-24-RGD. Nonetheless, both the autophagy inhibitor 3-MA and the autophagy inducer rapamycin had little effect on viral replication (Fig. 4). Collectively, these results indicate that autophagy correlates with cell lysis induced by the virus and that autophagosome formation is sufficient to disrupt the integrity of membrane structures in the cell. Fusion of the autophagosome with the lysosome is not necessary for the induction of efficient cell lysis by Delta-24-RGD.

Autophagy plays a role in adenovirus-mediated cell lysis. Atg5/Atg12 conjugation is an essential process in autophagy development (26). To examine the role autophagy plays in adenovirus-mediated cell lysis, we first took advantage of $ATG5^{-/-}$ MEFs for the study (11). After infection with Delta-24-RGD, in a dose-dependent manner, the virus induced autophagy only in wild-type (wt) but not in $ATG5^{-/-}$ MEFs, as indicated by conversion of LC3-I to LC3-II (Fig. 5A). Consistently, electron microscopy studies revealed numerous autophagic vacuoles in wt MEFs but only a few in $ATG5^{-/-}$ MEFs (Fig. 5B). Delta-24-RGD caused tremendous cell lysis in wt MEFs (~70% at 100 PFU/cell) but only modest cell death in $ATG5^{-/-}$ MEFs (~9% at 100 PFU/cell) (Fig. 5C and D). Consistently, Adwt also induced much less cell lysis in $ATG5^{-/-}$ MEFs than in wt MEFs (Fig. 5E). Although high doses of viruses were used in the experiments, UV-inactivated viruses at the highest dose did not cause any toxicity in the cells (Fig. 5E). It is unlikely that the cell lysis is caused by E1A toxicity since E1A expression is equivalent in both cell lines and since the level of cytolysis is so much lower in $ATG5^{-/-}$ cells (Fig. 5A). The cell lysis disparity is also not due to a lack of late gene expression in $ATG5^{-/-}$ MEFs since fiber protein expression actually accumulated in $ATG5^{-/-}$ MEFs, probably because of defective autophagic degradation of aggregated proteins (Fig. 5A). However, we did not observe assembled viral particles in the cells (data not shown). Next, we down-modulated the expression levels of proteins Atg5 and Atg10 (the ligase for Atg5 and Atg12 conjugation) (28) with shRNA against the genes encoding these proteins in human glioma U-87 MG cells (Fig. 6A). As indicated by decreased conversion of LC3-I to LC3-II, the shRNAs inhibited autophagy induction by Delta-24-RGD (Fig. 6B), resulting in efficient blockage of cell lysis (Fig. 6C). Taken together, these data demonstrate that autophagy plays a role in adenovirus-mediated cell lysis.

Autophagy-triggered caspase activity contributes to Delta-24-RGD-induced cell lysis. Since the Atg5-Atg12 conjugate was reported to be able to recruit FADD and caspase 8 to the membrane, resulting in activation of caspases and the transition from autophagy to autophagic cell death (33), we were interested in determining whether caspase activity is involved in adenovirus-induced cell lysis. For this purpose, we examined caspase activity in a set of leukemia cell lines: parental cell line A3 and its derivatives I2.1 with FADD deficiency and I9.2 with no caspase 8 expression (5). Although Delta-24-RGD induced autophagy in all three cell lines, as demonstrated by p62 degradation (Fig. 7A), caspase 8 was activated (cleaved caspase 8) only in A3 cells, not in the other two cell lines (Fig. 7A). The cleavage of lamin B1 and PARP1, substrates for caspase activity (19, 38), was increased only in A3 cells after viral infection as well (Fig. 7A). Consequently, both FADD and caspase 8 deficiencies were able to partially rescue infected cells from being lysed by the virus (Fig. 7B). The disparity was not due to the difference in infectivity levels in these cell lines because infection of the three cell lines with AdGFP-RGD resulted in similar GFP expression levels in the three cell lines (data not shown). To confirm the involvement of caspase activity in virus-mediated cell lysis, we then treated adenovirus-infected A3 cells with Z-VAD-Fmk (where Fmk is fluoromethyl ketone), a caspase inhibitor. Both caspase 8 and lamin B1 cleavage was prevented (Fig. 7C), resulting in a reduction of the amount of cell lysis by about 40% (Fig. 7D). However, the activation of caspases was not through the intrinsic pathway since the release of cytochrome *c* from the mitochondria to cytoplasm (23)

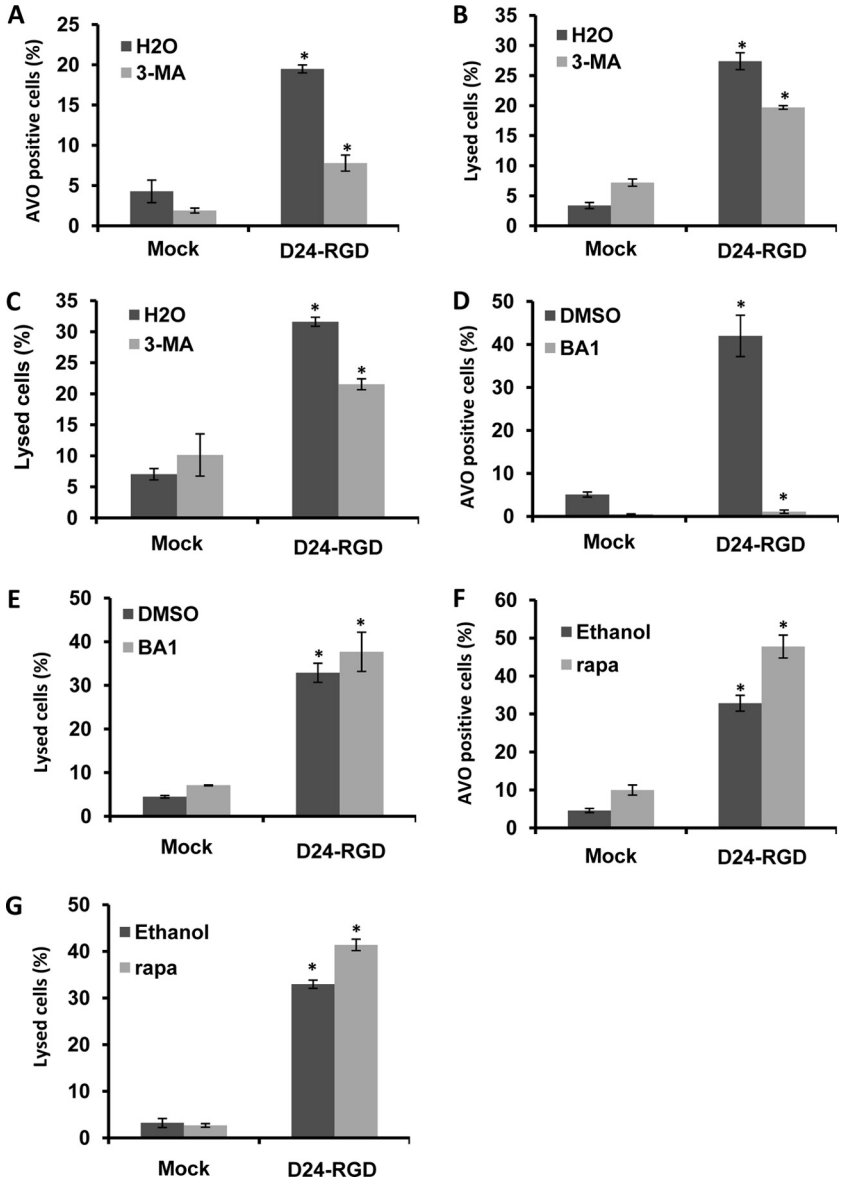

FIG. 3. Effect of autophagy modulators on Delta-24-RGD-induced autophagy and cell lysis in U-87 MG cells. Cells were infected with Delta-24-RGD at 10 PFU/cell. Twenty-four hours later, cells were treated with 5 mM 3-methyladenine (3-MA; A, B, and C) or 10 nM bafilomycin A1 (BA1; D and E); alternatively, 3 h later cells were treated with 1 μM rapamycin (Rapa; F and G). Forty-eight hours after viral infection, cells were assayed for acidic vesicle organelles (AVO); alternatively, at 72 h postinfection, cells were assayed for cell lysis. *P* values are indicated by asterisks as follows: 0.001 (A), 0.008 (B), 0.0007 (C), 0.005 (D), 0.07 (E), 0.009 (F), and 0.02 (G). Note that cell lysis in panels B, E, and G was assayed with ethidium homodimer 1 staining, and cells in panel C were assayed for cell lysis with trypan blue staining. Three independent experiments were performed. Data are shown as means ± SD. D24-RGD, Delta-24-RGD. H_2O, dimethyl sulfoxide (DMSO), or ethanol was used as a solvent for the 3-MA, BA1, or rapamycin, respectively.

was not detected after viral infection (Fig. 7E), which suggests that caspase activation was the result of the FADD/caspase 8 cascade. To determine the connection between adenovirus-induced autophagy and caspase activation, we infected wt and *ATG5*$^{-/-}$ MEFs with Delta-24-RGD. As expected, the virus caused much more caspase 8 and lamin B1 cleavage in wt MEFs than in *ATG5*$^{-/-}$ MEFs (Fig. 7F). Therefore, these data demonstrate that autophagy triggers caspase activity via the FADD/caspase 8 pathway and contributes to the cell lysis caused by Delta-24-RGD.

DISCUSSION

Advances in understanding how adenoviruses interact with host cells have led to the development of oncolytic adenoviruses that are currently being tested in clinical settings (16). We along with others have previously shown that cells infected with oncolytic adenoviruses undergo autophagy (12, 15). However, the functional relevance of autophagy in adenovirus-mediated cell lysis has not been examined. We speculate that vacuolization of the cytoplasm by the process of autophagy

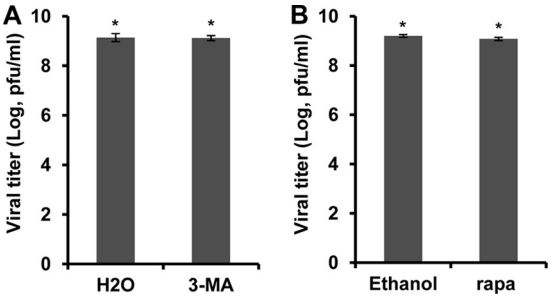

FIG. 4. Effect of autophagy modulators on Delta-24-RGD replication in U-87 MG cells. Cells were infected with Delta-24-RGD at 10 PFU/cell. Twenty-four hours later, cells were treated with 5 mM 3-methyladenine (3-MA) (A), or 3 h later cells were treated with 1 μM rapamycin (Rapa) (B). The titers of the viral progenies were determined 48 h after viral infection. Shown are the titers of viral progenies from 5×10^4 cells in 1 ml infected with the virus. The experiments were performed once in triplicate. Means ± SD are shown (*, $P > 0.05$). H_2O or ethanol was used as solvent for the 3-MA or rapamycin, respectively.

renders cells fragile and facilitates physical destruction of cellular structures, resulting in release of adenoviral progenies. Here, for the first time, we demonstrate that autophagy plays a role in the process of cell lysis induced by adenovirus. Importantly, our data reveal that autophagy-triggered caspase activity also contributes to adenovirus-induced cell lysis.

There are a few reports suggesting that adenoviral proteins regulate the cell lysis process. The L3 adenoviral protease cleaves cytokeratin 18 (K18), causing reorganization of the cellular skeleton that might promote host cell lysis and release of viral progeny (6). The E3 11.6-kDa adenovirus death protein (ADP), an integral membrane glycoprotein, facilitates destruction of the nuclear membrane and release of progeny virions (39, 40). Overexpression of ADP was reported to increase the oncolysis induced by adenoviruses (7). Whether these two proteins are involved in regulation of autophagy is unclear.

Nevertheless, our data clearly demonstrate that autophagy plays a role in adenovirus-mediated cell lysis. The virus can

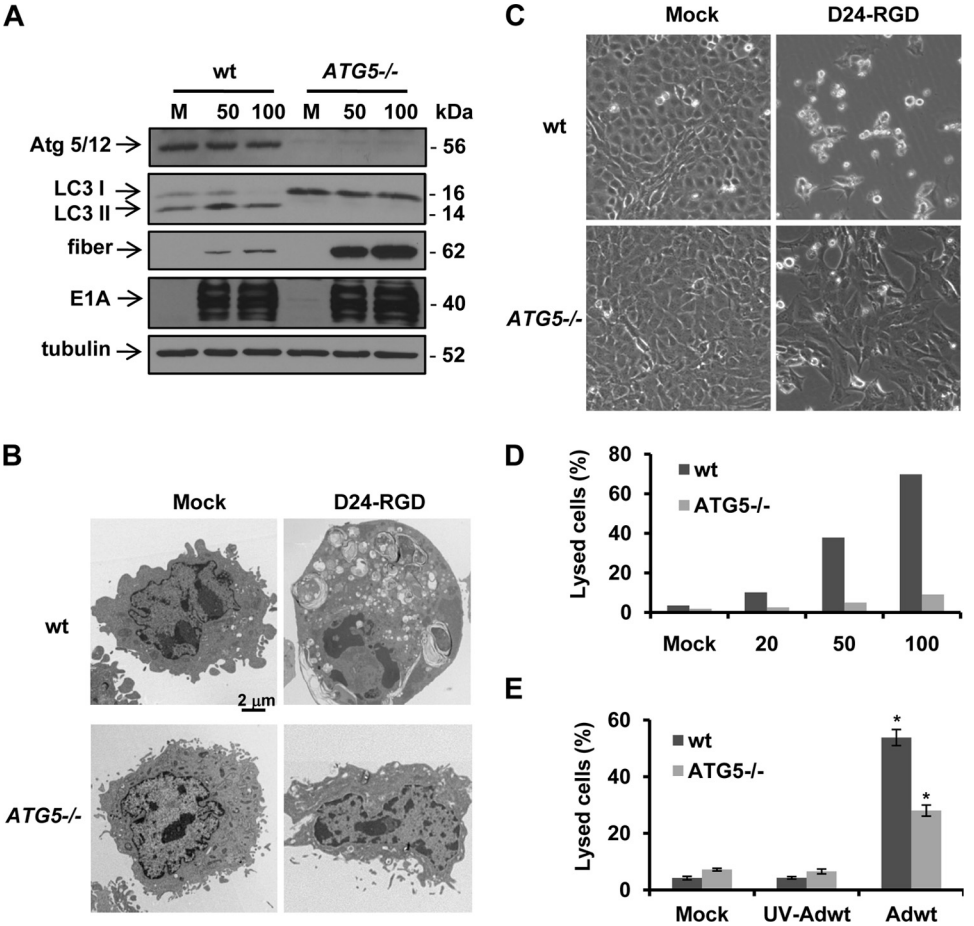

FIG. 5. *ATG5* knockout blocks adenovirus-induced autophagy and cell lysis in wild-type (wt) or *ATG5* knockout (*ATG5*$^{-/-}$) MEFs. (A) Cells were infected with Delta-24-RGD at the indicated doses (PFU/cell). After 72 h, cell lysates were collected for immunoblot analysis. Tubulin expression was used as a loading control. (B) Representative electron micrographs. Cells were infected with Delta-24-RGD at 50 PFU/cell for 72 h. Note that numerous vacuoles are induced by the virus in wt MEFs but only a few are induced in *ATG5*$^{-/-}$ MEFs. (C) Phase-contrast images of MEFs infected with Delta-24-RGD at 100 PFU/cell for 72 h. (D) Cell lysis caused by Delta-24-RGD in MEFs. Cells were infected with Delta-24-RGD at the indicated doses (PFU/cell). Seventy-two hours later, the cells were assayed for cell lysis. (E) Cells were infected with Adwt at 100 PFU/cell. Seventy-two hours later, the cells were assayed for cell lysis. Three independent experiments were performed. Data are shown as means ± SD. *, $P = 0.004$. M; mock; D24-RGD, Delta-24-RGD; UV-Adwt, UV-inactivated Adwt.

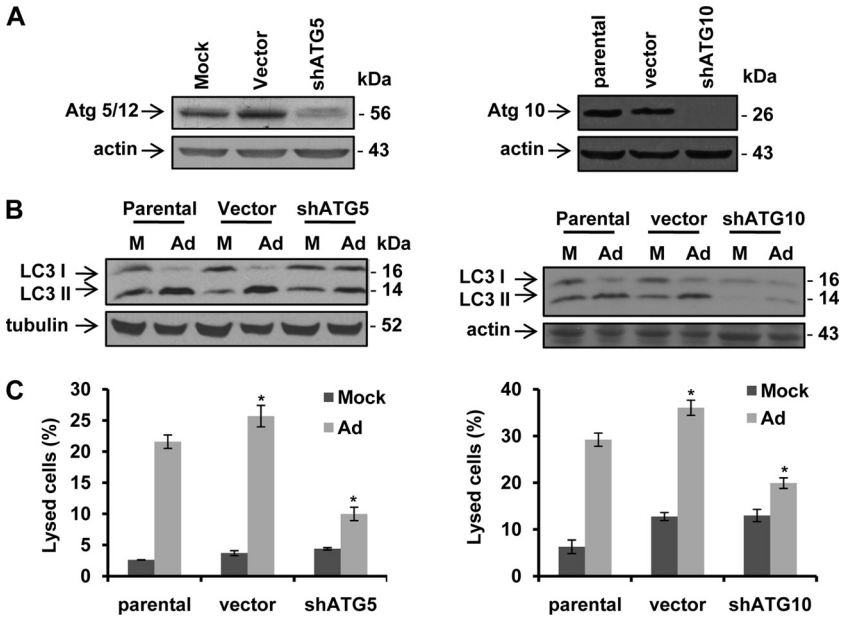

FIG. 6. shRNA against *ATG* genes inhibits Delta-24-RGD-induced autophagy and cell lysis in U-87-MG cells. (A) ATG5 or ATG10 expression in U-87-MG (parental cells), cells transfected with control vector, and cells transfected with plasmid expressing shRNA against *ATG5* (shATG5) or *ATG10* (shATG10). Cell proteins were analyzed by immunoblotting. Actin expression was used as a loading control. (B) shRNA against *ATG5* or *ATG10* inhibits autophagy induction by Delta-24-RGD. Cells were infected with Delta-24-RGD at 10 PFU/cell. Forty-eight hours later, cell lysates were collected and analyzed by immunoblotting. Tubulin or actin was used as a loading control. (C) shRNA against *ATG5* or *ATG10* rescues cells from lysis by Delta-24-RGD. Cells were infected with Delta-24-RGD at 10 PFU/cell. Seventy-two hours later, cells were assayed for cell lysis. Three independent experiments were performed. Data are shown as means ± SD (*, $P < 0.004$). M; mock; Ad, Delta-24-RGD.

induce a complete autophagy flux. However, since 3-MA but not bafilomycin A1 can rescue the cells from being lysed by Delta-24-RGD, it is reasonable to conclude that the membrane reorganization during autophagy is the one responsible for the destruction of the cellular structures. The fusion of the autophagosome with the lysosome is not relevant to the lysis process although the hydrolysases could degrade the contents within the membrane structure. Consistent with the above observations, knockout or downmodulation of the key autophagy gene *ATG5* substantially impairs the ability of the virus to induce lysis of host cells (Fig. 5 and 6). Downregulation of *ATG10* also shows the same effect (Fig. 6). In contrast, the autophagy inducer rapamycin enhanced Delta-24-RGD-induced autophagy and cell lysis (Fig. 3F and G). Thus, there is a cause-and-effect relationship between autophagy and efficient cell lysis. This suggests that autophagy, a highly genetically programmed cellular process, is a candidate target whose manipulation might improve the efficiency of oncolytic adenovirus to induce lysis in cancer cells.

The activation of caspases is indicated as a transition from autophagy to autophagic cell death (33). Our data show that caspases are activated in the context of adenovirus-induced autophagy and that this activation contributes to cell lysis (Fig. 7). Notably, caspase 8 activity is triggered through recruitment of FADD by Atg5/Atg12 to the membrane (33). Consistently, our data demonstrate that Delta-24-RGD increases caspase 8, PARP1, and lamin B1 cleavage only in parental leukemia A3 cells, not in cells without expression of FADD or caspase 8 (Fig. 7A). In *ATG5*$^{-/-}$ cells, moreover, Delta-24-RGD is unable to activate caspase 8 and displays diminished lamin B1 cleavage (Fig. 7F), indicating that autophagy is required for caspase 8 activation. The fact that no cytochrome *c* is released to the cytoplasm after adenoviral infection further confirms that the autophagy-triggered extrinsic pathway is the main factor in activation of caspases at the late stage of viral infection (Fig. 7E). We speculate that proteolysis of cellular structural proteins (such as lamin B1) by caspases collaborates with vacuolization by autophagy to destroy the host cellular structure and thus release viral progenies. Therefore, unlike the hydrolases from lysosomes, caspases contribute to the cell lysis induced by the virus. It looks as though what happens within the autophagic vacuoles (degradation by hydrolases) does not affect the lysis, but what happens outside the vacuoles (caspase activation) contributes to the lysis. However, the extent of the contribution depends on the status of the caspase activation pathways in the cells. In contrast to results in leukemia cells, we did not observe caspase activation in glioma cells after viral infection (data not shown). This is consistent with the previous report that glioma cells appear not to activate the extrinsic death receptor-dependent apoptotic pathway in response to irradiation or cytotoxic drugs (35). Thus, reactivating this pathway in glioma cells during viral infection could be another potential approach to improving oncolytic adenovirus potency.

Our results here also provide a mechanistic rationale for our previous reports showing that rapamycin has a synergistic effect with oncolytic adenoviruses and strongly suggest that rapamycin-enhanced oncolytic potency is, at least in part, due to facilitation of autophagy (2). These findings suggest that oncolytic adenoviruses could be combined advantageously with drugs that induce autophagy, including, importantly, temozolomide, the gold standard of glioma treatment. In this regard,

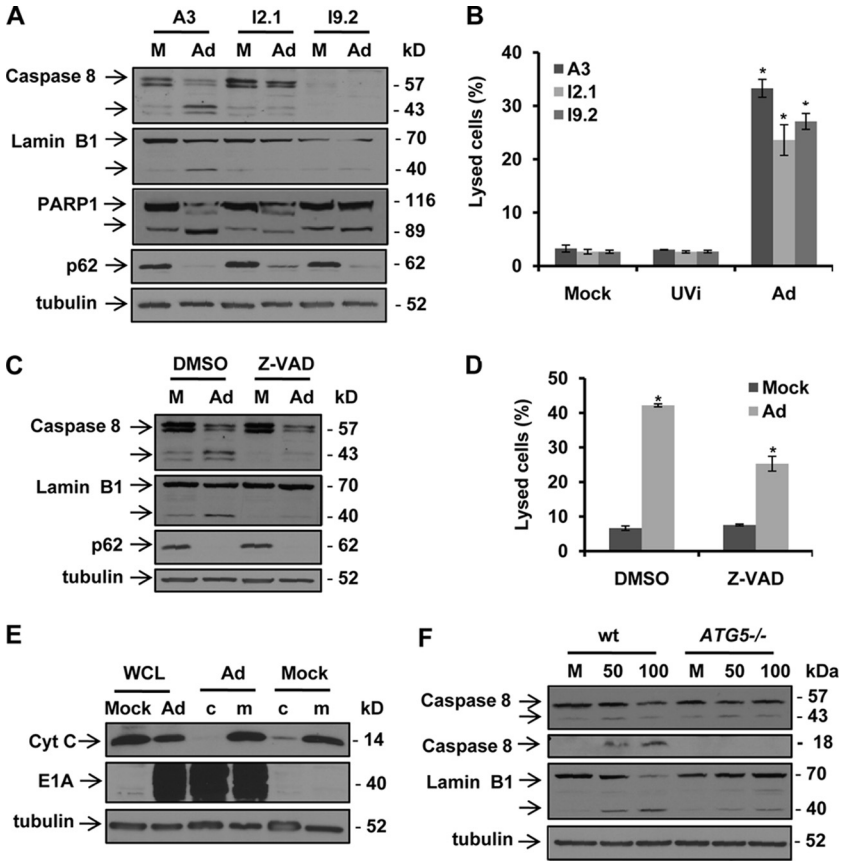

FIG. 7. Autophagy-triggered caspase activity contributes to Delta-24-RGD-induced cell lysis. (A) Induction of autophagy and caspase activation by Delta-24-RGD. Human leukemia cell lines A3 (parental), I2.1 (FADD-null), and I9.2 (caspase 8-null) were infected with Delta-24-RGD at 100 PFU/cell. Seventy-two hours later, cell lysates were analyzed by immunoblotting. Tubulin expression was used as a loading control. (B) Cell lysis caused by Delta-24-RGD. Cells were treated as described for panel A and were assayed for cell death. Three independent experiments were performed. Data are shown as means ± SD (*, $P < 0.05$). (C) Inhibition of caspase activation by Z-VAD-Fmk. A3 cells were infected with Delta-24-RGD at 100 PFU/cell. Twenty-four hours later, 50 μM Z-VAD-Fmk was added to the cells. After 48 h, cell lysates were analyzed by immunoblotting. Tubulin expression was used as a loading control. (D) Z-VAD-Fmk rescues cells from lysis by Delta-24-RGD. A3 cells were treated as described for panel C. Cells were assayed for cell death. Three independent experiments were performed. Data are shown as means ± SD (*, $P = 0.007$). (E) Delta-24-RGD does not cause cytochrome *c* (Cyt C) release to the cytoplasm. A3 cells were infected with Delta-24-RGD at 100 PFU/cell. Seventy-two hours later, proteins from the cytosol (c) and mitochondria (m) were extracted from the cells and analyzed by immunoblotting. Tubulin expression was used as a loading control. (F) Atg5 is required for caspase activation. MEFs were infected with Delta-24-RGD at the indicated doses (PFU/cell). Seventy-two hours later, cell lysates were analyzed with immunoblotting. Tubulin expression was used as a loading control. M, mock; Ad, Delta-24-RGD. UVi, UV-inactivated Delta-24-RGD.

temozolomide induces autophagy and has synergistic effects with oncolytic adenoviruses (44).

In summary, we demonstrate here that autophagy plays a role in adenovirus-mediated cell lysis. It triggers caspase activity for collaborative lysis of host cells. Of further clinical relevance, our study provides a new mechanism for adenovirus-induced cell lysis through which strategies can be imposed to improve oncolytic adenoviral potency in cancer therapy.

ACKNOWLEDGMENTS

This work was supported by a National Institutes of Health P50 award (CA127001) and core grant CA16672 to The University of Texas M. D. Anderson Cancer Center and by a grant from the Marcus Foundation (to J. Fueyo).

We thank Kathryn Hale (Department of Scientific Publications, The University of Texas M. D. Anderson Cancer Center) for editorial assistance, and Kenneth Dunner, Jr., for electron microscopy analysis (High Resolution Electron Microscopy Facility, The University of Texas M. D. Anderson Cancer Center).

REFERENCES

1. **Abou El Hassan, M. A., I. van der Meulen-Muileman, S. Abbas, and F. A. Kruyt.** 2004. Conditionally replicating adenoviruses kill tumor cells via a basic apoptotic machinery-independent mechanism that resembles necrosis-like programmed cell death. J. Virol. **78:**12243–12251.
2. **Alonso, M. M., et al.** 2008. Delta-24-RGD in combination with RAD001 induces enhanced anti-glioma effect via autophagic cell death. Mol. Ther. **16:**487–493.
3. **Baehrecke, E. H.** 2005. Autophagy: dual roles in life and death? Nat. Rev. Mol. Cell Biol. **6:**505–510.
4. **Berk, A. J.** 2007. *Adenoviridae*: the viruses and their replication, 5th ed., vol. II. Lippincott Williams & Wilkins, Philadelphia, PA.
5. **Bodmer, J. L., et al.** 2000. TRAIL receptor-2 signals apoptosis through FADD and caspase-8. Nat. Cell Biol. **2:**241–243.
6. **Chen, P. H., D. A. Ornelles, and T. Shenk.** 1993. The adenovirus L3 23-kilodalton proteinase cleaves the amino-terminal head domain from cytokeratin 18 and disrupts the cytokeratin network of HeLa cells. J. Virol. **67:**3507–3514.
7. **Doronin, K., et al.** 2000. Tumor-specific, replication-competent adenovirus vectors overexpressing the adenovirus death protein. J. Virol. **74:**6147–6155.
8. **Fass, E., E. Shvets, I. Degani, K. Hirschberg, and Z. Elazar.** 2006. Microtubules support production of starvation-induced autophagosomes but not their targeting and fusion with lysosomes. J. Biol. Chem. **281:**36303–36316.

9. **Fueyo, J., et al.** 2003. Preclinical characterization of the antiglioma activity of a tropism-enhanced adenovirus targeted to the retinoblastoma pathway. J. Natl. Cancer Inst. **95:**652–660.
10. **Fueyo, J., et al.** 2000. A mutant oncolytic adenovirus targeting the Rb pathway produces anti-glioma effect in vivo. Oncogene **19:**2–12.
11. **Hosokawa, N., Y. Hara, and N. Mizushima.** 2007. Generation of cell lines with tetracycline-regulated autophagy and a role for autophagy in controlling cell size. FEBS Lett. **581:**2623–2629.
12. **Ito, H., et al.** 2006. Autophagic cell death of malignant glioma cells induced by a conditionally replicating adenovirus. J. Nat. Cancer Inst. **98:**625–636.
13. **Ito, H., S. Daido, T. Kanzawa, S. Kondo, and Y. Kondo.** 2005. Radiation-induced autophagy is associated with LC3 and its inhibition sensitizes malignant glioma cells. Int. J. Oncol. **26:**1401–1410.
14. **Jackson, W. T., et al.** 2005. Subversion of cellular autophagosomal machinery by RNA viruses. PLoS Biol. **3:**e156.
15. **Jiang, H., et al.** 2007. Examination of the therapeutic potential of Delta-24-RGD in brain tumor stem cells: role of autophagic cell death. J. Natl. Cancer Inst. **99:**1410–1414.
16. **Jiang, H., F. McCormick, F. F. Lang, C. Gomez-Manzano, and J. Fueyo.** 2006. Oncolytic adenoviruses as antiglioma agents. Expert Rev. Anticancer Ther. **6:**697–708.
17. **Jiang, H., E. J. White, C. Gomez-Manzano, and J. Fueyo.** 2008. Adenovirus's last trick: you say lysis, we say autophagy. Autophagy **4:**118–120.
18. **Jones, N., and T. Shenk.** 1978. Isolation of deletion and substitution mutants of adenovirus type 5. Cell **13:**181–188.
19. **Kivinen, K., M. Kallajoki, and P. Taimen.** 2005. Caspase-3 is required in the apoptotic disintegration of the nuclear matrix. Exp. Cell Res. **311:**62–73.
20. **Klionsky, D. J.** 2007. Autophagy: from phenomenology to molecular understanding in less than a decade. Nat. Rev. Mol. Cell Biol. **8:**931–937.
21. **Kuma, A., et al.** 2004. The role of autophagy during the early neonatal starvation period. Nature **432:**1032–1036.
22. **Levine, B.** 2005. Eating oneself and uninvited guests: autophagy-related pathways in cellular defense. Cell **120:**159–162.
23. **Li, H., H. Zhu, C. J. Xu, and J. Yuan.** 1998. Cleavage of BID by caspase 8 mediates the mitochondrial damage in the Fas pathway of apoptosis. Cell **94:**491–501.
24. **Lindmo, K., and H. Stenmark.** 2006. Regulation of membrane traffic by phosphoinositide 3-kinases. J. Cell Sci. **119:**605–614.
25. **Mahasreshti, P. J., et al.** 2001. Adenovirus-mediated soluble FLT-1 gene therapy for ovarian carcinoma. Clin. Cancer Res. **7:**2057–2066.
26. **Mizushima, N., et al.** 1998. A protein conjugation system essential for autophagy. Nature **395:**395–398.
27. **Mizushima, N., and T. Yoshimori.** 2007. How to interpret LC3 immunoblotting. Autophagy **3:**542–545.
28. **Mizushima, N., T. Yoshimori, and Y. Ohsumi.** 2002. Mouse Apg10 as an Apg12-conjugating enzyme: analysis by the conjugation-mediated yeast two-hybrid method. FEBS Lett. **532:**450–454.
29. **Orvedahl, A., and B. Levine.** 2008. Viral evasion of autophagy. Autophagy **4:**280–285.
30. **Paglin, S., et al.** 2001. A novel response of cancer cells to radiation involves autophagy and formation of acidic vesicles. Cancer Res. **61:**439–444.
31. **Pankiv, S., et al.** 2007. p62/SQSTM1 binds directly to Atg8/LC3 to facilitate degradation of ubiquitinated protein aggregates by autophagy. J. Biol. Chem. **282:**24131–24145.
32. **Petiot, A., E. Ogier-Denis, E. F. Blommaart, A. J. Meijer, and P. Codogno.** 2000. Distinct classes of phosphatidylinositol 3′-kinases are involved in signaling pathways that control macroautophagy in HT-29 cells. J. Biol. Chem. **275:**992–998.
33. **Pyo, J. O., et al.** 2005. Essential roles of Atg5 and FADD in autophagic cell death: dissection of autophagic cell death into vacuole formation and cell death. J. Biol. Chem. **280:**20722–20729.
34. **Rubinsztein, D. C., J. E. Gestwicki, L. O. Murphy, and D. J. Klionsky.** 2007. Potential therapeutic applications of autophagy. Nat. Rev. Drug Discov. **6:**304–312.
35. **Steinbach, J. P., and M. Weller.** 2004. Apoptosis in gliomas: molecular mechanisms and therapeutic implications. J. Neurooncol. **70:**247–256.
36. **Suzuki, K., R. Alemany, M. Yamamoto, and D. T. Curiel.** 2002. The presence of the adenovirus E3 region improves the oncolytic potency of conditionally replicative adenoviruses. Clin. Cancer Res. **8:**3348–3359.
37. **Suzuki, K., et al.** 2001. A conditionally replicative adenovirus with enhanced infectivity shows improved oncolytic potency. Clin. Cancer Res. **7:**120–126.
38. **Tewari, M., et al.** 1995. Yama/CPP32 beta, a mammalian homolog of CED-3, is a CrmA-inhibitable protease that cleaves the death substrate poly(ADP-ribose) polymerase. Cell **81:**801–809.
39. **Tollefson, A. E., J. S. Ryerse, A. Scaria, T. W. Hermiston, and W. S. Wold.** 1996. The E3-11.6-kDa adenovirus death protein (ADP) is required for efficient cell death: characterization of cells infected with *adp* mutants. Virology **220:**152–162.
40. **Tollefson, A. E., et al.** 1996. The adenovirus death protein (E3-11.6K) is required at very late stages of infection for efficient cell lysis and release of adenovirus from infected cells. J. Virol. **70:**2296–2306.
41. **Ulasov, I. V., et al.** 2009. Combination of adenoviral virotherapy and temozolomide chemotherapy eradicates malignant glioma through autophagic and apoptotic cell death in vivo. Br. J. Cancer **100:**1154–1164.
42. **Wileman, T.** 2006. Aggresomes and autophagy generate sites for virus replication. Science **312:**875–878.
43. **Xie, Z., and D. J. Klionsky.** 2007. Autophagosome formation: core machinery and adaptations. Nat. Cell Biol. **9:**1102–1109.
44. **Yokoyama, T., et al.** 2008. Autophagy-inducing agents augment the antitumor effect of telerase-selve oncolytic adenovirus OBP-405 on glioblastoma cells. Gene Ther. **15:**1233–1239.